PAPER

Dual-wavelength mode-locked fiber laser based on tungsten disulfide saturable absorber

IOP Publishing | Astro Ltd Laser Physics

Laser Phys. **27** (2017) 125802 (5pp) https://doi.org/10.1088/1555-6611/aa9143

Dual-wavelength mode-locked fiber laser based on tungsten disulfide saturable absorber

Xiaowen Li[1], Jianqiang Qian[1], Ruwei Zhao[2], Fan Wang[3] and Zhenyu Wang[1]

[1] Department of Applied Physics, Key Laboratory of Micro-nano Measurement-Manipulation and Physics (Ministry of Education), Beihang University, Beijing 100191, People's Republic of China
[2] State Key Laboratory of Crystal Materials, Institute of Crystal Materials, Shandong University, Jinan 250100, People's Republic of China
[3] Faculty of Science, Department of Physics and Astronomy, ARC Centre for Nanoscale BioPhotonics, Macquarie University, Sydney, NSW 2109, Australia

E-mail: qianjq@buaa.edu.cn

Received 26 June 2017, revised 26 September 2017
Accepted for publication 3 October 2017
Published 22 November 2017

Abstract

We report on the generation of dual-wavelength mode-locked laser pulse in an Er-doped ring-shaped fiber cavity with WS_2 nanosheets based saturable absorber (SA), emitting at wavelength of 1531.8 nm and 1556.7 nm. The WS_2 nanosheets were precipitated on the head face of fiber patch cord via light precipitation method. By adjusting the polarization of lasing mode, the gain of the Er-doped fiber laser was effectively controlled and the stable dual-wavelength mode-locking operation was achieved. Our investigation revealed WS_2's extraordinary nonlinear properties, which make it an excellent material for saturable absorber for passively mode-locked fiber lasers.

Keywords: tungsten disulfide, saturable absorber, dual-wavelength mode-locked, fiber ring cavity, erbium doped fiber laser

(Some figures may appear in colour only in the online journal)

1. Introduction

Due to their wide applications in optic communication, industry material processing, frequency comb and biomedical researches [1–3], ultrafast pulse fiber lasers based on different materials and configurations have been attracting an increasing amount of attention in a verity of research fields. Passively mode locking is a well-known method to generate ultrafast pulses [4], including multi-wavelength mode-locking pulses. Numerous types of mode-locking devices, such as Kerr lens [5], nonlinear polarization rotation (NPR) [6, 7] and semiconductor saturable absorber mirror (SESAM) [8], have been used to obtain stable multi-wavelength mode-locking pulses in fiber lasers. However, in previous studies, the output wavelength was selected by optical filtering [9, 10], and in most cases the maximum spacing between the output wavelengths were merely a few nanometers, which limited the capability and application of multi-wavelength mode-locking lasers.

Recently, two-dimensional (2D) materials have been widely used to generate ultrafast laser pulses [11–20]. Among them, molybdenum disulfide (MoS_2), due to its high third order nonlinearity, has been applied utilized in advanced laser applications [11–14]. Tungsten disulfide (WS_2), a member of 2D semiconducting transition metals dichalcogenides (TMDCs) family, exhibits ultrafast nonlinear saturable absorption property and has high optical damage threshold [15]. WS_2 has a stackable S–W–S (S: sulfur atom, W: tungsten atom) molecular structure, which provides very strong hexagonally bone between S and W, and van der waals forces based interaction between each layers. Those structures indicate unique electronic and optoelectronic properties [15], such as valley polarization, strong spin–orbit effect, high surface-to-volume ratio and integrated circuits with logic operation that has enabled various applications.

In 2015, Mao *et al* [16] demonstrated that at the pump power of 600 mW, WS_2 saturable absorbers could work

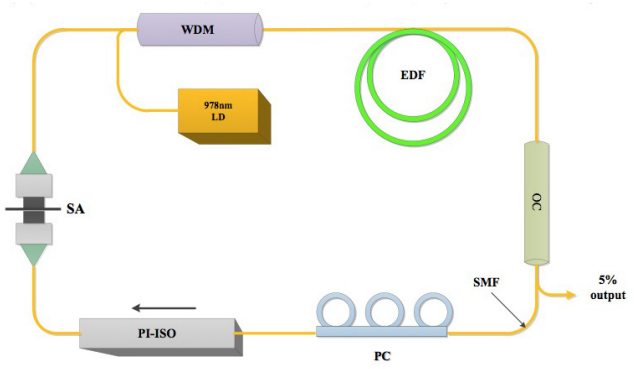

Figure 1. Passively mode-locked fiber laser cavity schematic (WDM: wavelength division multiplexer, SA: saturable absorber, PC: polarization controller, EDF: erbium-doped fiber).

stably in the soliton mode-locking state without damage. They concluded that WS_2 nanosheets have the ultrafast nonlinear saturable absorption property and a high optical damage threshold. Yan *et al* [17] investigated a new type of microfiber-based WS_2 saturable absorber. At the pump power of 675 mW, they obtained harmonic mode-locking laser pulses with up to 1 GHz repetition rate. The pulse duration is 452 fs while the signal-to-noise ratio is 48 dB. By depositing WS_2 onto the surface of the tapered fiber, Khazaeniezhad *et al* [18] demonstrated that reducing the waist diameter of the tapered fiber induced an increase in the spectral bandwidth of the ultrafast pulses, and reduced the bandwidth to 3 dB. In another study [19], they generated a saturable absorber by growing multiple layers of WS_2 on a two-side-polished fiber via chemical vapor deposition (CVD) method, which in turn was used to generate stable soliton-like pulses with a spectral width of 5.6 nm and a 467 fs's pulse duration. In these studies, benefits of strong nonlinear optical responses in WS_2 were fully utilized, and various kinds of single-wavelength mode-locking operation were achieved. However, few studies about multi-wavelength mode-locking operations have been reported.

In this study, a WS_2 SA was exposed to a passively-mode-locked all-fiber laser near 1550 nm which in turn generated dual-wavelength mode-locked pulse train. The WS_2 nanosheets were precipitated onto the head face of fiber patch cord via light precipitation method. A ring-shaped fiber cavity was built to generate pulse trains. Their characteristics were explored and compared in the following sections.

2. Experimental setup

We constructed a ring cavity fiber laser and inserted the WS_2 saturable absorber (SA) to achieve passive mode locking. The experimental setup is presented in figure 1. The total length of fiber in this ring cavity fiber laser is approximately 120 m, including 8 m C-band erbium-doped fiber (EDF, Nufern, M5-980-125) as gain medium with a dispersion parameter of ~ -12.2 ps (km • nm)$^{-1}$ and a peak absorption of 6.2 dB m^{-1} at 1530 nm as well as 110 m standard single mode fiber (SMF) with dispersion parameter of 18 ps (km • nm)$^{-1}$. The total net cavity dispersion is ~1.01 ps^2. A 978 nm semiconductor laser with 500 mW maximum output power provides pump through a 980/1550 nm wavelength division multiplexer (WDM). A polarization-independent isolator (PI-ISO) at the end of the amplifier section is employed to maintain unidirectional operation and a polarization controller (PC) is employed to adjust the mode-locking state. Light is extracted from the cavity through a direction coupler with 10% output coupling ratio, and then monitored via a digital oscilloscope (Tektronix DPO7104), an optical spectrum analyzer (Yokogamo AQ7370B) and a radio frequency (RF) spectrum analyzer (Agilent N9320A).

3. Experimental results and discussion

3.1. Characterization of WS_2 saturable absorber

There are two popular methods for the manufacture of 2D materials: The first is micromechanical exfoliation technique, which has been widely used to prepare single- and few-layer 2D materials nanosheets. However this method is not applicable for mass production [15, 20]. The second method is chemical vapor deposition (CVD), which requires expensive equipment [21]. Compared with the above two methods, liquid-phase preparation (LPE) is efficient at synthesizing wafer-scale thin films in large quantity and thus is regarded as a promising method for the manufacture of composite materials [11].

In this experiment, WS_2 nanosheets were synthesized via LPE method. To prepare the sample, WS_2 nanosheets were exfoliated from thick slices and dispersed into water by sonication. Then LiOH as the stabilizer was added to stabilize them. The dispersions are stable over tens of days. As shown in figure 2(a), the prepared WS_2 dispersions showed a dark brown color. The lateral sizes of the WS_2 nanosheets were measured with an ultra-high resolution scanning electron microscope (SEM) on a silicon substrate with 1 nm resolutions, as shown in figure 2(b). Figure 2(c) shows the WS_2 nanosheets' Raman spectrum which was measured with 532 nm laser. The typical Raman peaks of WS_2 can be clearly observed in the figure, with the in-plan phonon modes E^1_{2g} at 349.8 cm^{-1} and the out-of-plan phonon modes A_{1g} at 418.2 cm^{-1}. This phenomenon had been discussed in the earlier researches [22]. In figure 2(d), the linear optical absorption spectrum and the transmission spectrum of WS_2 nanosheets were measured via UV–VIS–NIR spectrophotometer, the blue line shows a less obvious absorption peak at 609 nm, which arises from a direct band-gap transition at the K point [23]. The red line also shows an obvious dip also at 609 nm on the transmission spectrum which could be attributed to the direct gap transmission.

According to a previous study [24], by introducing defects, the bandgap of MoS_2 could be reduced to 0.26 eV. It can be inferred that defects in WS_2 nanosheets, because of the similarity between material properties of WS_2 and MoS_2, has similar effects. In our experiment, WS_2 SA was prepared by light precipitation method, and WS_2 nanosheets were of various shapes. Because the direct bandgap of monolayer WS_2 is about 2.0 eV (630 nm) [25, 26], the saturable absorption near 1550 nm belongs to sub-bandgap absorption.

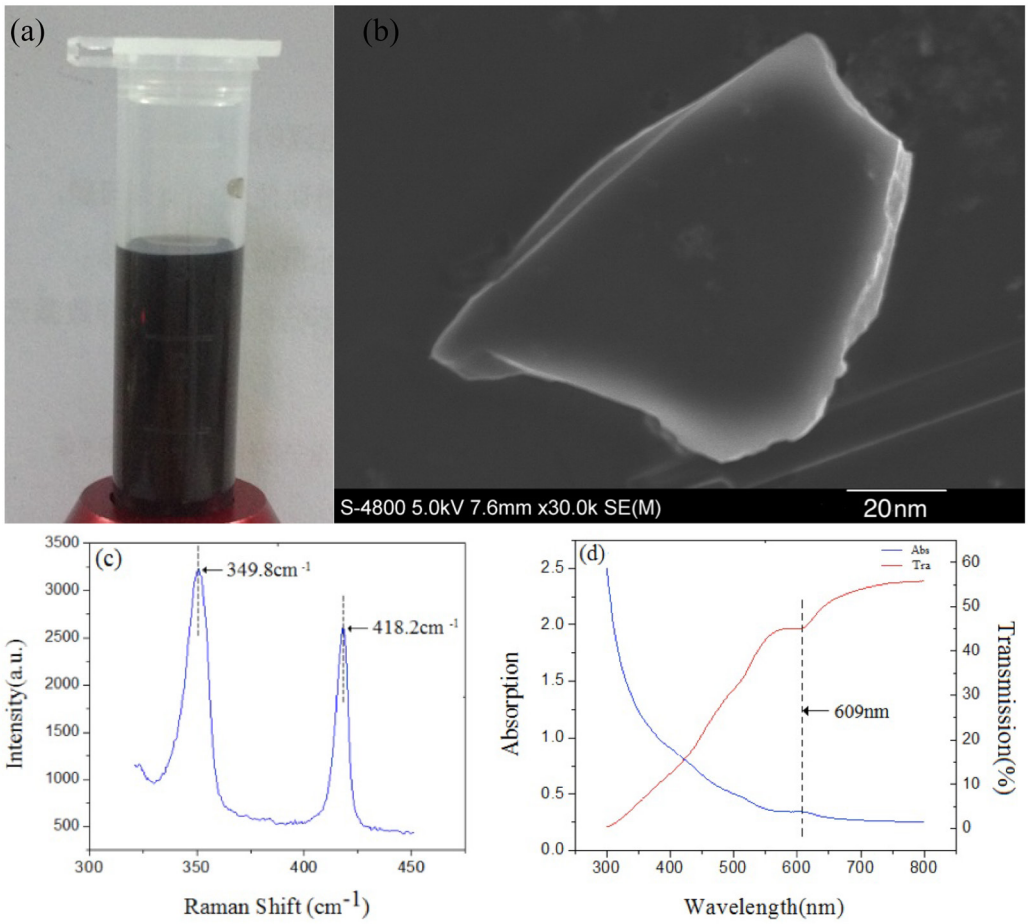

Figure 2. Characterization of WS_2 nanosheets: (a) image of WS_2 dispersion; (b) SEM image of WS_2 nanosheets on silicon substrate; (c) Raman spectrum of WS_2 nanosheets on silicon substrate; (d) linear optical absorption and transmission spectrum of WS_2 nanosheets.

3.2. Dual-wavelength mode locking

In our experiment, the stable dual-wavelength mode-locking pulses were achieved by properly adjusting the PC. To obtain ultrafast pulses, the pump power was gradually increased to the mode-locking threshold. The output pulses of the fiber lasers showed very high stability, which was proved by the radio frequency (RF) spectrum. The measured repetition rates were in good agreement with the design parameters of the cavity.

To confirm the stable mode-locking operation, a 1 GHz photodetector and a 2.5 GHz real-time oscilloscope were employed to investigate the pulse train in time domain. The results are presented in figures 3(a) and (b), in witch very uniform pulse amplitude can be observed. The uniform amplitudes in turn prove that the laser was operating in the continuous wave mode-locking state. The pulse interval was 600 ns which matched with the laser cavity round trip time. This verified the mode-locking operation of the fiber laser.

The laser output properties are summarized in figure 4(a) which shows the spectrum of dual wavelength mode-locking pulses. There are obviously two peaks respectively located at 1531.8 nm and 1556.7 nm with a 3 dB bandwidth of ~2.8 nm and ~1.9 nm. Theoretically, there are also many weeny wave crests distributed on both sides of the two main wave crests, but due to the low resolution of spectrometer, those

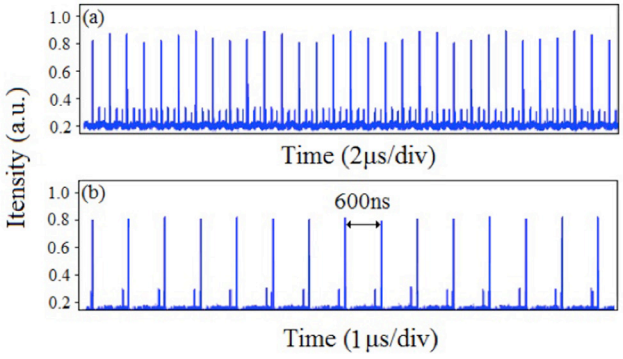

Figure 3. Oscilloscope trace of the laser: (a) mode locking pulse train at pump power of 100 mW, (b) single-pulse mode locking.

microstructure of main wave crests are invisible to us. To investigate the stability of dual-wavelength mode-locking pulses, we measured its RF spectrum, which is shown in figure 4(b). The fundamental repetition frequency is 1.65 MHz, with the signal-to-noise ratio being up to ~60 dB. This matches exactly with the pulse train's periods and the estimated fundamental frequency of the implemented ring cavity. Notably, only one peak was observed in RF. Furthermore, its RF spectrum was measured in a wider range (200 KHz), as shown in the inset of figure 4(b). The dual-wavelength mode-locking pulse exhibits relatively good long-term stability. The picosecond pulses

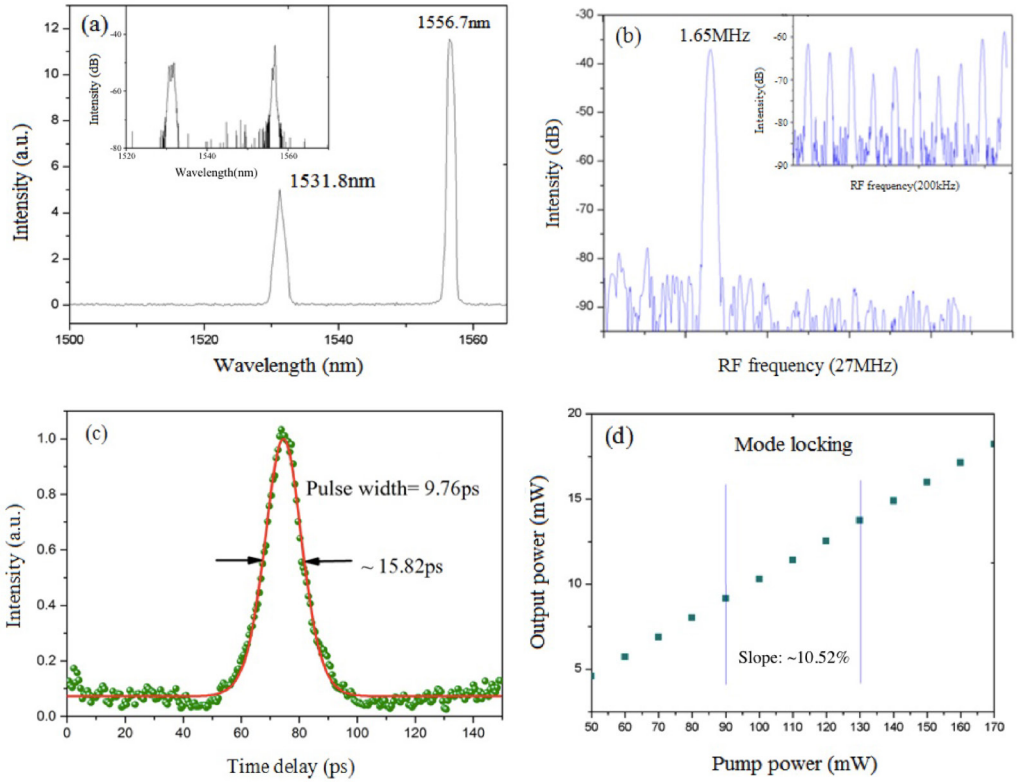

Figure 4. Passively mode-locking laser performance at pump power of 100 mW: (a) optical spectrum, (b) RF spectrum of fundamental frequency, (c) auto-correlation trace, (d) output power with respect to pump power of the mode-locked laser based on WS_2 SA.

were measured via auto-correlation methods which yielded a full width at half maximum width (FWHM) of 15.82 ps. Consequently, the pulse duration τ was 9.76 ps under the assumption of a $sech^2$ pulse profile, as shown in figure 4(c). Figure 4(d) shows a typical dual-wavelength mode-locking pulse train which would be observed when the output power of the ring cavity with WS_2 SA was 8.97 mW with a pump power being 90 mW. The mode locking can be sustained at the pump power ranging from ~90 mW to 130 mW. The maximum output power of laser is 13.74 mW with the pulse energy of ~8.31 nJ and the light conversion efficiency up to ~10.52%. At the maximum pump power of 130 mW, mode-locking operation can be maintained for several hours as long as the experiment condition remains unchanged.

The mechanism of dual-wavelength mode-locking operation in our fiber laser can be described by the following process. When the cavity loss reaches some specific values, the gain of the Er-doped fiber and the cavity loss will have nearly equal magnitudes, which further, combining with the high nonlinear effect of the WS_2 SA [27], makes the dual-wavelength mode-locking operation feasible. Additionally, to test whether the WS_2 SA contributed to the passive mode-locking, we replaced the WS_2 SA with new fiber patch cord without WS_2. No dual-wavelength mode-locking was observed, even after we changed pump power continuously from zero to the maximum (500 mW) and adjusted the PC over a full range. After WS_2 SA was inserted into cavity, dual-wavelength mode-locking pulse could be observed again. The comparison proved that the dual-wavelength mode-locking pulse was caused by WS_2 SA rather than the NPR effect.

4. Conclusions

In conclusion, we constructed a passively-mode-locked Er-doped fiber laser and investigated the optical characteristics of WS_2. The WS_2 SA was prepared by light precipitation method. Stable dual-wavelength mode-locking pulse train with emission wavelengths of 1531.8 nm and 1556.7 nm, was obtained. Its pulse duration was 9.76 ps and had a repetition rate of 1.65 MHz. The maximum output power of the laser was 13.74 mW and pulse energy was of ~8.31 nJ. This investigation indicated that as a SA material, WS_2 had excellent nonlinear performance for applications in passively mode-locked fiber lasers. Substantial enhancement in this 2D materials performance can be expected with further optimization of the SA fabrication together with the laser cavity designing.

Acknowledgments

This work at Beihang University was supported by Beijing Natural Science Foundation (4132038).

References

[1] Keller U 2003 Recent developments in compact ultrafast lasers *Nature* **424** 831–8
[2] Sohn I B, Kim Y S, Noh Y C, Ryu J C and Kim J T 2009 Microstructuring of optical fibers using femtosecond laser *J. Opt. Soc. Korea* **13** 33–6
[3] Letokhov V S 1985 Laser biology and medicine *Nature* **316** 325–30

[4] Sutter D H, Steinmeyer G, Gallmann L, Matuschek N, Morier-Genoud F, Keller U, Scheuer V, Angelow G and Tschudi T 1999 Semiconductor saturable-absorber mirror assisted Kerr-lens mode-locked Ti:sapphire laser producing pulses in the two-cycle regime *Opt. Lett.* **24** 631–3

[5] Wu J, Cai H, Han X H and Zeng H P 2008 Multi-pulse operation of a Kerr-lens mode-locked femtosecond laser *Chin. Opt. Lett.* **6** 76–8

[6] Feng X, Tam H Y and Wai P K 2006 Stable and uniform multi wavelength erbium-doped fiber laser using nonlinear polarization rotation *Opt. Express.* **14** 8205–10

[7] Matsas V J, Newson T P, Richardson D J and Payne D N 1992 Selfstarting passively mode-locked fibre ring soliton laser exploiting nonlinear polarisation rotation *Electron. Lett.* **28** 1391–3

[8] Keller U, Weingarten K J, Kartner F X, Kopf D, Braun B, Jung I D, Fluck R, Honninger C, Matuschek N and Aus der Au J 1996 Semiconductor saturable absorber mirrors (SESAM's) for femtosecond to nanosecond pulse generation in solid-state laser *IEEE J. Sel. Top. Quantum Electron.* **2** 435–53

[9] Luo Z C, Luo A P, Xu W C, Yin H S, Liu J R, Ye Q and Fang Z J 2010 Tunable multiwavelength passively mode-locked fiber ring laser using intracavity birefringence-induced comb filter *IEEE Photon. J.* **2** 571–7

[10] Zhang H, Tang D Y, Wu X and Zhao L M 2009 Multi-wavelength dissipative soliton operation of an erbium- doped fiber laser *Opt. Express* **17** 12692–7

[11] Coleman J N *et al* 2011 Two-dimensional nanosheets produced by liquid exfoliation of layered materials *Science* **331** 568–71

[12] Mak K F, Lee C, Hone J, Shan J and Heinz T F 2010 Atomically thin MoS_2: a new direct-gap semiconductor *Phys. Rev. Lett.* **105** 136805

[13] Najmaei S, Liu Z, Zhou W, Zou X, Shi G, Lei S, Yakobson B I, Idrobo J-C, Ajayan P M and Lou J 2013 Vapour phase growth and grain boundary structure of molybdenum disulphide atomic layers *Nat. Mater.* **12** 754–9

[14] Chhowalla M, Shin H S, Eda G, Li L-J, Loh K P and Zhang H 2013 The chemistry of two-dimensional layered transition metal dichalcogenide nanosheets *Nat. Chem.* **5** 263–75

[15] Wang Q H, Strano M S, Kalantar-Zadeh K, Kis A and Coleman J N 2012 Electronic and optoelectronics of two-dimensional transition metal dichalcogenides *Nat. Nanotechnol.* **7** 699–712

[16] Mao D, Wang Y, Ma C, Han L, Jiang B, Gan X, Hua S, Zhang W, Mei T and Zhao J 2015 WS_2 mode-locked ultrafast fiber laser *Sci. Rep.* **5** 7965

[17] Yan P *et al* 2015 Microfiber-based WS_2-film saturable absorber for ultra-fast photonics *Opt. Mater. Express* **5** 479

[18] Khazaeinezhad R, Kassani S H, Jeong H, Yeom D-I and Kyunghwan O 2015 Femtosecond soliton pulse generation using evanescent field interaction through tungsten disulfide (WS_2) film *J. Lightwave Technol.* **33** 3550–7

[19] Khazaeinezhad R, Kassani S H, Jeong H, Park K J and Kim B Y 2015 Ultrafast pulsed all-fiber laser based on tapered fiber enclosed by few-layer WS_2 nanosheets *IEEE Photon. Technol. Lett.* **27** 1581–4

[20] Radisavljevic B, Radenovic A, Brivio J, Giacometti V and Kis A 2011 Single-layer MoS_2 transistors *Nat. Nanotechnol.* **6** 147–50

[21] Cong C, Shang J, Wu X, Cao B, Peimyoo N, Qiu C, Sun L and Yu T 2013 Synthesis and optical properties of large-scale single-crystalline two-dimensional semiconductor WS_2 monolayer from chemical vapor deposition *Adv. Opt. Mater.* **2** 131–6

[22] Berkdemir A *et al* 2013 Identification of individual and few layers of WS_2 using Raman spectroscopy *Sci. Rep.* **3** 1755

[23] Zhao W, Ghorannevis Z, Chu L, Toh M, Kloc C, Tan P H and Eda G 2013 Evolution of electronic structure in atomically thin sheets of WS_2 and WSe_2 *ACS Nano* **7** 791–7

[24] Huang Y, Luo Z, Li Y, Zhong M, Xu B, Che K, Xu H, Cai Z, Peng J and Weng J 2014 Widely-tunable, passively *Q*-switched erbium-doped fiber laser with few-layer MoS_2 saturable absorber *Opt. Express* **22** 25258–66

[25] Fu X, Qian J, Qiao X, Tan P and Peng Z 2014 Nonlinear saturable absorption of vertically stood WS_2 nanoplates *Opt. Lett.* **39** 6450–3

[26] Khazaeizhad R, Kassani S H, Jeong H, Yeom D I and Oh K 2014 Mode-locking of Er-doped fiber laser using a multilayer MoS_2 thin film as a saturable absorber in both anomalous and normal dispersion regimes *Opt. Express* **22** 23732–42

[27] Wang G, Zhang S, Zhang X Y, Zhang L, Cheng Y, Fox D, Zhang H Z, Coleman J N, Blau W J and Wang J 2015 Tunable nonlinear refractive index of two-dimensional MoS_2, WS_2, and $MoSe_2$ nanosheets dispersions *Photon. Res.* **3** A51–5